capstract:2611.00027v1 [physics.ao-ph] 16 Nov 2026

Recovery of buoyancy-driven exchange in a repeatedly opened cold reservoir

Elin A. Nyström-Lago,[1,*] Daisuke M. Arakawa-Luz,[2] and Nadia Belhadri-Mercier[1,3]

[1] *Laboratory for Environmental Flow, Toftesund Technical Institute, Aarhus, Denmark*
[2] *Department of Geophysical Fluid Dynamics, Kawanose Institute of Science, Sendai, Japan*
[3] *Centre de Circulation Atmosphérique, Institut de Veyrac, Toulouse, France*

(Dated: November 16, 2026)

Repeated openings of a finite cold-air reservoir need not admit equal amounts of sensible heat. We measure the heat entering a $\mathbf{0.280\,m^3}$ enclosure through a full-height aperture during pairs of identical openings separated by sealed intervals of 6 to 240 s. At an initial temperature deficit of 18 K, the second opening admits $\mathbf{0.49}$ times the heat of the first after 6 s (95% confidence interval 0.46 to 0.52) and $\mathbf{0.99}$ times after 240 s (0.96 to 1.02). An event model based on the relaxation of the air temperature following isolated openings predicts the dependence on the sealed interval without adjustment to the paired data. Velocity profiles show a weaker outflow at short intervals, although the sign reversal at the aperture remains close to midheight. A heat budget bounds the contribution of wall storage, and isothermal controls characterize the flow driven by the hinge motion. For fixed contents and a prescribed opening trajectory, the thermal load per inspection depends on the time since the previous inspection even when the outcome is identical.

I. INTRODUCTION

Air leaving a shallow cold reservoir forms a gravity current. When the exit spans the full depth, the flow along the floor is accompanied by a return flow at greater height. A zero net volume flux can coexist with substantial heat transport. This mechanism appears in natural ventilation [1] and in the surface outflows produced by atmospheric cold pools [2]. A difference between those settings is the supply of dense air. With no source at the aperture and a finite stock behind it, the mouth can continue to pass fluid well after the densest fluid available to export has gone.

Lock-exchange experiments describe the resulting front and its dependence on the initial density contrast [3, 4]. The head is three dimensional and exchanges fluid with its surroundings [5]. For thermal budgets, the front's speed and position are less informative than the velocity and temperature on the aperture itself. A model for ventilation through a vertical partition uses the same aperture balance [6]. In refrigerated spaces, the balance has usually been tested against exchange during one opening or averaged over enough openings that the system's history enters as an operating condition [7, 8].

An isolated opening starts from an interior state to which the reservoir has had time to return. When the reservoir is opened again soon after closure, the opening motion can be reproduced while the initial thermal state cannot. Estimating second-opening heat from total open time leaves both openings with the same weight. Estimating it from the temperature at a single point is also problematic. A probe near the floor can miss air replaced higher up. Prior experiments with repeated ventilation of weakly forced enclosures describe this dependence on probe location [9]. We use volume-integrated temperature measurements to construct the pre-opening state and aperture data to measure the heat independently.

The reservoir in this experiment is a domestic refrigerator with its shelves, bins, and contents removed. We use a repeatable opening trajectory corresponding to a brief visual inspection of the compartment. The single-opening runs establish the initial exchange and the subsequent recovery, and paired runs test whether the recovery of air temperature alone predicts the additional load at a second inspection. Section II develops the corresponding event map. Sections III and IV give the measurement procedure and the comparison.

II. MODEL

A. Aperture exchange

Let T_o be the external air temperature and $\bar{T}$ the volume mean air temperature inside the enclosure. The baseline interior temperature is T_b, with deficit $D_0 = T_o - T_b$. During a run, $D = T_o - \bar{T}$. At the aperture let u_n be positive out of the cabinet. We use the Boussinesq approximation at reference density ρ_0 and write the net sensible heat gain during opening j as

$$Q_j = \rho_0 c_p \int_{I_j}\int_{A(t)} u_n(\mathbf{x},t)[T_o(t) - T(\mathbf{x},t)]\, dA\, dt. \quad (1)$$

The reference temperature removes the nearly canceling enthalpy transports of the counterflows. An outgoing parcel colder than the room contributes positively to Q_j. A returning parcel from a previous discharge can be colder than the room and makes a negative contribu-

* elin.nystrom-lago@toftesund.example

tion, a distinction that matters when the second opening starts before the first current has dispersed. The aperture area $A(t)$ excludes the part still covered by the moving door. The time window I_j extends from the first detectable clearance at the seal to the reestablishment of contact.

For constant density within each compartment and a neutral plane at midheight, integrating the hydrostatic velocity from the sill to the neutral plane gives the one-way volume flux scale

$$\dot{V}_b = \frac{C_d}{3} W H \sqrt{g' H}, \qquad g' = g D_0 / T_m, \tag{2}$$

where W and H are aperture width and height, $T_m = (T_o + T_b)/2$ in kelvin, and C_d is a discharge coefficient [6]. The estimate presumes two deep reservoirs. In the cabinet the interior deficit decreases over a single opening. A neutral plane set by a single height is also approximate while the door is in motion. We use Eq. (2) to choose an opening long enough to exchange an observable fraction of the air.

For $W = 0.48$ m, $H = 0.66$ m and $D_0 = 18.0$ K at $T_m = 286$ K, the reduced gravity is $0.62\,\mathrm{m\,s^{-2}}$. The aperture velocity scale is $0.64\,\mathrm{m\,s^{-1}}$ and the time to travel one aperture height at this speed is about 1 s. With $C_d = 0.6$ the flux is about $0.040\,\mathrm{m^3\,s^{-1}}$. Over 5.7 s at full opening, it could displace $0.23\,\mathrm{m^3}$, comparable to the cabinet volume of $0.280\,\mathrm{m^3}$. The nominal Reynolds number $H\sqrt{g'H}/\nu$ is about 2.8×10^4 for $\nu = 1.5 \times 10^{-5}\,\mathrm{m^2\,s^{-1}}$. A well-mixed enclosure with this flux would replace about $1 - \exp(-0.23/0.280) \simeq 0.56$ of its initial temperature deficit during the dwell alone. Displacement favors faster removal of cold air, whereas the decline in the driving pressure during the opening favors slower removal. This estimate leaves the net replacement fraction to be measured.

B. Sealed recovery and the second opening

Define the dimensionless temperature anomaly $x = (\bar{T} - T_b)/D_0$, positive for an interior warmer than baseline. The first opening starts at $x = 0$. It leaves $x = f$, the fraction of the initial temperature deficit lost by closure. With the cabinet sealed we approximate the excess heat transfer to the cold surfaces by $G(\bar{T} - T_b)$, where G is an effective conductance. Subtracting the steady heat balance and taking the air heat capacity $C_a = \rho_0 c_p V$ gives

$$C_a \frac{dx}{dt} = -G x, \qquad x(t) = f \exp(-t/\tau), \qquad \tau = C_a/G. \tag{3}$$

Here t is measured from closure. The expression for G absorbs the influence of internal circulation. The inferred conductance applies to the time range and baseline wall conditions used in the experiment. A cold wall returning from a temperature excursion generates a second time scale, as observed in small sealed chambers after heating pulses [10]. The measurements in Sec. III track that excursion separately.

We approximate the aperture heat for a prescribed opening trajectory by $Q(D) = qD$, where q is an empirical heat per unit pre-opening deficit, with units of J/K. This approximation follows exactly if the trajectory replaces a fixed fraction of the air deficit and concurrent wall storage scales with D. In the cabinet q and f are obtained from different observations, so that the agreement of qD_0 with $C_a f D_0$ is an energy-budget check. Both q and f could in principle depend on D. The linear approximation treats the opening as a short event; the subsequent sealed recovery enters through x at the start of the next event.

For a pair of identical openings separated by Δ, the first starts at deficit D_0 and the second at $D_0[1 - x(\Delta)]$. The predicted ratio is

$$R(\Delta) \equiv \frac{Q_2}{Q_1} = 1 - f \exp(-\Delta/\tau). \tag{4}$$

The predicted dependence on interval in Eq. (4) comes entirely from the thermal transient in a single-opening run. At long gaps the two openings have the same expected heat. At gaps small compared with τ, the second starts with a deficit of approximately $(1 - f)D_0$. This limit still represents two complete door motions. A door held open for twice as long has a different kinematic boundary condition. The experiment excludes gaps below 6 s, in part because the airflow generated by closure still occupies the threshold region at earlier times.

The one-way flux in Eq. (2) varies as $D^{1/2}$, so an alternative limiting model retains this dependence throughout an opening of duration t_a. If the interior mixes instantaneously, the deficit obeys $dD/dt = -kD^{3/2}$ and

$$Q(D) = C_a D \left[1 - \left(1 + k t_a \sqrt{D}/2 \right)^{-2} \right]. \tag{5}$$

It gives a stronger reduction in Q_2 as the initial deficit shrinks. The premise of instantaneous mixing is restrictive in a shallow cabinet. Natural ventilation can preserve vertical segregation even when the throughflow itself is turbulent [11, 12]. We use Eq. (5) as a comparison at short gaps. The experiment was designed to distinguish this case from Eq. (4) over the measured interval, without attempting to infer an exponent for general aperture geometries.

III. EXPERIMENT

A. Reservoir and chamber

The cabinet occupied one end of a $4.8 \times 4.0 \times 2.9\,\mathrm{m}$ chamber. Its sill was 0.07 m above the chamber floor. The next obstacle in the path of the floor current was the far wall, 3.8 m from the sill. Side clearance was 1.1 m or greater. During acquisition, air conditioning supplied the chamber through a high-level diffuser behind the cabinet. At rest the air speed 0.3 m in front of the opening was below $0.03\,\mathrm{m\,s^{-1}}$. We measured this quantity near the sill and midheight, where a background crossflow would alter the inferred neutral height. Concurrent wind and buoyancy can make comparable contributions when this speed approaches the aperture scale [13]. Here the ratio was below 0.05 when the cabinet began at its full deficit.

A liquid-cooled plate fitted flush to the rear of the liner maintained the cold boundary. The original door, gasket, and hinge remained in place. The plate temperature was controlled with a circulating bath outside the chamber. The cabinet fan and interior lamp were disconnected. No air was drawn through the cabinet during the sealed interval. The temperature of the cabinet was therefore regulated without a fan pulse or lamp pulse synchronized to the door.

Temperature set points for valid runs were $22.0\,^{\circ}\mathrm{C}$ in the chamber and $4.0\,^{\circ}\mathrm{C}$ for the volume mean inside, each within 0.2 K before the first opening. The coldest monitored liner position stayed above $1.5\,^{\circ}\mathrm{C}$. The room dew point was $-6 \pm 1\,^{\circ}\mathrm{C}$, measured with a chilled mirror. This separation reduced latent heat transfer. It also held the density difference mainly to its thermal component. A constant $\rho_0 = 1.22\,\mathrm{kg\,m^{-3}}$ and $c_p = 1006\,\mathrm{J\,kg^{-1}\,K^{-1}}$ were used for Eq. (1).

A motor drove the door from the closed position to 80 degrees in 0.65 s, held it there for 5.70 s, then closed it in 0.65 s. A contact encoder gave both endpoints. The opening trajectory varied by less than 0.03 s between runs. A fixed camera at the side of the chamber recorded the view of the compartment. In pilot runs the lower velocity measurements were sensitive to movement in front of the door. During acquisition the operator remained behind a partition.

B. Thermometry and velocity

Air temperature inside the cabinet was sampled by 36 fine-wire junctions, one per cell of a $4 \times 3 \times 3$ volume grid. The front row lay clear of the aperture to avoid biasing the inferred interior temperature toward the counterflow. The baseline and the sealed recovery used the same volume weights. The junctions were calibrated together at three temperatures spanning the range of the runs. Mean relative error between junctions after correction was 0.05 K. A step-response bench measurement gave a junction time constant of 0.12 ± 0.02 s in the aperture flow range. We applied a first-order lag correction at the aperture. In the sealed interior, where local velocity was largely unknown, we evaluated that correction as an uncertainty term and started the recovery fit 2 s after closure.

Stereoscopic particle image velocimetry gave the normal velocity through the aperture at 100 frames per second [14]. The reconstruction plane was at the shoulder of the sill. The opening mask followed the door angle. A separate temperature grid with eight columns and ten heights provided temperatures interpolated to the velocity mesh. Temperature and velocity were interpolated to common times using a synchronization pulse recorded by both systems. The pointwise product in Eq. (1) retains the covariance of velocity and temperature during acceleration and closure.

The aperture grid was finer normal to the mean height of the counterflow separation than at the extreme upper and lower edges. Those edges required extrapolation over the first or last half-cell. We used a no-penetration boundary value at the edge with interpolation to the innermost measured node. Below 12 degrees the door itself blocked the illuminated plane at a small fraction of the locations that were geometrically open. The flux there was estimated from time interpolation between zero at closure and the first angle with full coverage. Replacing that interpolation with zero, or with an extrapolation from the first resolved two frames, supplied the edge and motion uncertainty in Table II. The convention for net volume drift and a check against cabinet air storage are detailed in Appendix A.

C. Protocol and estimators

Each of 12 daily blocks contained one isolated opening and one pair at each sealed interval $\Delta \in \{6, 15, 30, 60, 120, 240\}$ s. We permuted the seven run types independently within blocks, using a schedule generated before acquisition. The minimum separation between the end of a run and the beginning of the next was 900 s. We also required the baseline difference between cabinet and chamber to fall back to its acceptance window and the mean of the monitored liner temperatures to stay within 0.15 K of its reference value for 60 s. The latter check prevented a run with restored air temperature but warm boundary surfaces from being treated as equilibrated. All 84 scheduled runs met the pre-opening limits and were retained. The wait between openings within a pair followed the assigned interval regardless of temperature.

We also made 12 zero-deficit trials with the plate held at room temperature, one after each block had finished and the plate had equilibrated to the chamber. This control measured a door-driven velocity pulse under the same trajectory. Its heat integral was evaluated against the same external reference. A further undisturbed record of 240 s at the beginning of each cold block established the baseline variability of the enclosure and the drift of the optical zero. Neither control contributed to the fitted recovery curve.

The primary observation for a pair was the within-run ratio $r_{b,d} = Q_{2,b,d}/Q_{1,b,d}$ for day b and assigned delay d. We report the arithmetic mean of the 12 ratios at each delay with pointwise Student intervals across blocks. Each delay contributes one independent daily value per block. An aggregate ratio of the two means gives more weight to days on which the first opening was large. We report the latter calculation as a sensitivity check.

We fitted Eq. (3) by least squares to the 2 to 240 s temperature record of each isolated opening, using time points 2, 4, 6, 10, 15, 22, 30, 45, 60, 90, 120, 180, and 240 s. Spreading the points in time prevents the many samples near baseline from setting the overall fit. The fitted amplitude was extrapolated back to the closure. We averaged the 12 fitted amplitudes and time constants and used their block variation for the reported calibration intervals. Prediction Eq. (4) uses those two means. The paired runs did not enter those fits. Resampling days intact, with their isolated run and six pairs kept together, was used for a secondary check on the difference between the prediction and the observations [15]. The tabled intervals for R reflect measurement repeatability, with systematic components treated separately in Table II.

IV. RESULTS

A. Flow at the opening

The first opening produced an outward flow below $z/H \simeq 0.53$ and an inward flow above it during the middle of the dwell (Fig. 1). The profile at the 6 s second opening retains the change of sign but has a smaller peak speed in both layers. At 240 s the measured profile is close to the first-opening profile. The transition from outflow to inflow spans several measurement cells. A two-layer fit with a sharp interface overestimates the speed near the reversal and increases the inferred transport. Entrainment across a continuously stratified shear layer can account for a finite thickness [16]. The profile alone gives limited information about how much of the mixing occurs inside the cabinet and how much occurs at the opening.

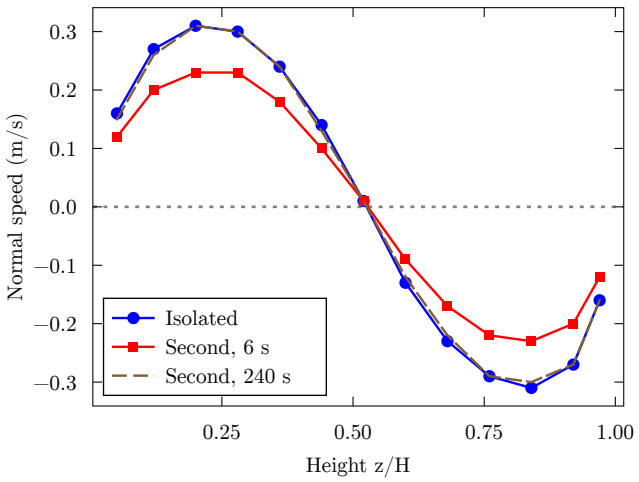


FIG. 1. Width-averaged normal air speed over the middle 2 s of the dwell, with positive values directed out of the cabinet. The first opening is from the 12 isolated runs. The 6 s and 240 s curves are second openings from the corresponding 12 pairs each.

The zero-deficit control resolved outward and inward peaks synchronized with the door's motion, as occurs in warmer ventilated enclosures with a swinging boundary [17]. In the control the width-averaged speed stayed below $0.03\,\mathrm{m\,s^{-1}}$ during the central dwell and the integrated heat was 0.01 kJ (95% confidence interval -0.03 to 0.05 kJ). Door-driven motion is present in every cold trial, but its duration and sign change differ from those of the buoyant exchange. Subtracting the neutral-control speed would assume superposition of the two flows. We retain the directly observed transport in the cold run.

Optical records outside the aperture showed the first current moving away along the chamber floor. An array of three ambient thermometers within 0.5 m of the sill registered a cold remnant during the 6 s and 15 s intervals. At 6 s it extended above the sill but lay below the height at which most of the supply flow entered the cabinet. Including the measured temperature of incoming parcels in Eq. (1), instead of assigning them room temperature, lowered the mean short-gap ratio by 0.01. The resulting ratio accounts for the heat actually entering the enclosure, regardless of when the incoming air last passed through its aperture.

B. Recovery from an isolated opening

The 12 isolated runs admitted a mean Q_1 of 3.59 kJ (95% confidence interval 3.50 to 3.68 kJ) at the aperture. For $V = 0.280\,\mathrm{m^3}$ the air heat capacity is 344 J/K. Multiplying by D_0 gives a full deficit of 6.19 kJ. The fitted amplitude $f = 0.58$ (95% confidence interval 0.56 to 0.60) puts about 3.59 kJ in the warmed air at

closure. The direct increase obtained from the interior probes at closure was 3.56 kJ. The temperature comparison and the flux estimate use different sensor grids and therefore provide a useful check on the magnitude of the measured exchange. At that point the interior still held about 2.6 kJ of its initial sensible deficit.

The fitted mean relaxation time was 54 s (95% confidence interval 49 to 60 s). This corresponds to an effective conductance of 6.4 W/K. At the first measured gap of 6 s the air retains most of the temperature anomaly left by the initial opening. At 120 s the anomaly is about 0.065 of the initial deficit. In Fig. 2 the last three points have similar absolute uncertainties. Dividing them by the fitted anomaly to evaluate relative error would give the noisy baseline undue influence. The positive residual at 240 s is within the variability of the measured baseline in the sealed control.

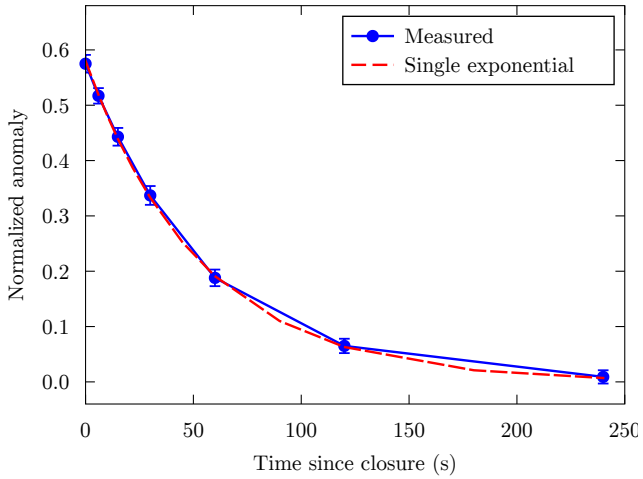


FIG. 2. Volume-mean interior temperature anomaly after one isolated opening, divided by the 18 K starting deficit. Points show means of 12 isolated runs. Error bars are pointwise 95% intervals over runs. The dashed line uses the mean fitted amplitude and time constant.

At 2 s after closure the warmest air was concentrated in the upper third of the enclosure. A probe in that layer gave a recovery amplitude about 0.14 higher than the volume mean when normalized by the initial deficit. A probe near the floor gave an amplitude about 0.12 lower. The aggregate relaxation time in Eq. (3) therefore depends on the measurement of the interior as a whole. The mean of the liner probes increased by 0.16 K by the end of the isolated opening, then changed by less than another 0.15 K over the first minute. Its full excursion during the recovery stayed below 0.35 K. This observation supports the fixed-boundary approximation for short gaps. It leaves room for a weak slow mode, which we cannot estimate precisely with a 240 s record.

C. Heat of the second opening

At 6 s the second opening admits approximately half the sensible heat of the first. The measured means increase with delay across the six settings (Table I). The prediction using f and τ from the isolated runs differs from the paired means by at most 0.011 after rounding. The shortest tested gap has the largest absolute difference from equal heat. The 240 s interval includes one, consistent with near recovery. Individual ratios exceed one in several of those runs. We retain them because the first heat in a pair is itself a measurement with error and day-to-day conditions can leave the second event cooler than the first.

TABLE I. Sensible heat ratio by sealed interval. Each observed mean and pointwise 95% confidence interval uses one pair per day for 12 days. The last column is Eq. (4) with coefficients fitted to the isolated runs.

Interval (s)	Mean	95% CI	Predicted
6	0.49	0.460 to 0.520	0.481
15	0.55	0.518 to 0.582	0.561
30	0.66	0.625 to 0.695	0.667
60	0.81	0.776 to 0.844	0.809
120	0.93	0.895 to 0.965	0.937
240	0.99	0.956 to 1.024	0.993

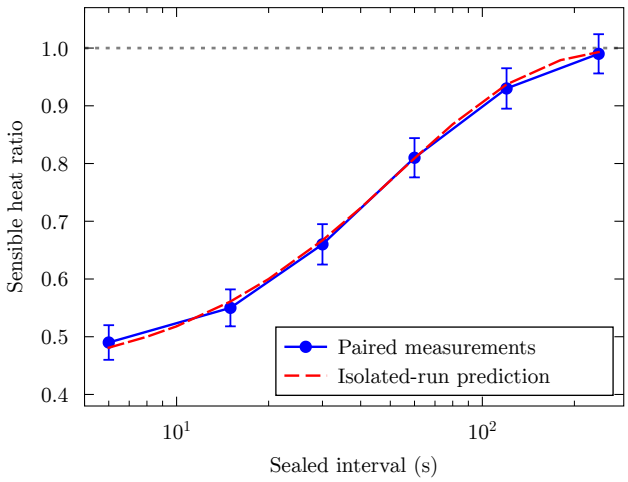


FIG. 3. Second-opening sensible heat divided by the first-opening heat in the same pair. Points and error bars give means and pointwise 95% intervals across daily blocks. The dashed curve is the prediction from isolated openings. The dotted line marks equal loads.

Normalizing by the first opening leaves the comparison largely insensitive to the common gain of the velocity and temperature measurements. In Fig. 3 a difference of 0.01 in either direction from the curve is small relative to the random error bars. It is also within the estimated residual calibration uncertainty on a ratio.

The aggregate ratio, calculated by averaging the component heats before division, changed the point estimates by at most 0.01. A bootstrap over entire daily blocks gave pointwise intervals on the prediction residuals that included zero at each gap. The comparison is a check of scale and timing. Modest curvature in the dependence of Q on the deficit remains plausible.

For Eq. (5), using the isolated-opening mean to set the bracketed term at D_0 to 0.58 gives $kt_a\sqrt{D_0}/2 = 0.54$ after rounding. The fractional pre-opening deficit at 6 s from Eq. (3) is 0.481. Using that deficit in Eq. (5) predicts $R \simeq 0.39$. The lower value comes from reducing the exchange rate as well as the initial deficit. Agreement with the linear model across our intervals suggests that some of the heat originates from the displacement of coherent layers, or from door-driven exchange that continues at weak thermal contrast. The present measurements do not uniquely separate those mechanisms. The profile in Fig. 1 shows that a smaller characteristic velocity can coexist with an approximately constant effective fraction of the cold inventory removed.

V. DISCUSSION

A finite stock of cold air introduces a memory into the event sequence. There are two simple ways to lose it in data reduction. The first sums opening duration within a reporting period and assigns the same flux to each second of equivalent open area. With a fixed opening trajectory that procedure would give an estimated load of $2Q_1$ for every pair. The measured average ratio at 6 s instead gives an average pair load of $1.49Q_1$ on a scale that sets each first opening to one. The second procedure starts the measurement at the moment a motor receives a command, counts the interval from there, and places the next command at Δ. For the 6 s condition this time convention would place the second command before the first closure. An interval intended to represent recovery must start at the end of the first exchange. Similar endpoint choices affect analyses of cavity and room measurements when a door-state log supplies the only timing [18].

The expectation for a second opening of a refrigerator whose contents cannot change is unusually clean. For each of our 72 pairs, the first opening provided a complete view of the empty compartment. The second opening confirmed the same occupancy. It nevertheless drew heat from the room. The threshold flow responds to the previous opening because it has removed cold air, and its recovery is set by the return of that air deficit, irrespective of what was observed inside. Field studies that code consecutive openings as separate retrievals from a door switch alone cannot distinguish these cases [19].

The air in a loaded enclosure would occupy a smaller accessible volume. Its passages would have different widths and the exposed contents would add thermal capacity with separate response times. Packing would also change the range of visible positions. These differences restrict the applicability of the measured ratios to an empty cabinet under the tested aperture motion and initial conditions. Two enclosures with the same Δ/τ can exchange different fractions of their starting deficits. Outdoor cold pools also differ because radiant heating, surface exchange, natural lateral boundaries, and evolving moisture change their density even without a repeat aperture event. Their profiles illustrate how a finite cold-air source drives an outflow, while the chamber permits an imposed return toward the source state.

The experiment assigns heat in the air to the particular opening that admitted it. Electrical demand is a different quantity. A refrigeration cycle integrates the heat withdrawn from air, liner and any stored material. The drive and chamber cooling in our apparatus are separate from this balance. The uncertainty in the total energy of a later compressor cycle would be dominated by the unknown phase of its controller and the heat stored in the surrounding structure. Neither is necessary to measure the thermal cost of a second confirmation in this apparatus.

VI. CONCLUSION

When an inspection leaves both the contents and the aperture schedule fixed, a change in the thermal state can still alter the heat of the next inspection. Matching the initial temperature reading at one height would allow much of that dependence to survive a nominal reset. A volume mean sampled before each opening is a more direct state variable. For scheduled sequences longer than a pair, wall recovery and persistent air outside the sill become candidates for additional state variables. An equivalent count of openings would then require those states or a controlled resetting interval. An inventory log that records the same empty compartment twice contains neither.

APPENDIX A: APERTURE INTEGRATION AND HEAT BUDGET

We represented each observed aperture cell by its projected open area. For each frame, we computed an outward volume residual by summing the signed area-weighted normal velocities. Integration over the full interval gave a mean residual of $0.006\,\mathrm{m}^3$ for the isolated openings, or 2% of the cabinet volume. This residual includes uncertainties close to the hinge and departures

from the equal-density model. A correction for optical velocity offset was estimated from the static reference images before each run, leaving the net volume residual free to vary during exchange. Forcing the volume residual to zero frame by frame would redistribute flux near the neutral level, where a small velocity correction can change the assigned sign of a cell.

The systematic uncertainty from imperfect mass balance was estimated by repeating the integral with the measured velocities adjusted uniformly in each open frame to have zero net volume. The range of changes in the resulting Q was compared with the correction calculated by using ideal-gas densities evaluated separately in each cell. Uncertainty in aperture interpolation was assessed by omitting alternate grid locations and repeating the computation using the coarser grid. We tested the response correction by varying the junction time constant within its bench uncertainty. These changes perturb the two heat integrals in a pair together. Treating the gain and lag of the two openings as independent would misrepresent their contributions to the uncertainty of the ratio.

At fixed cabinet volume, let H_w be the integrated rate of sensible transfer from air into solid surfaces during a single opening. The air balance is

$$Q_1 = C_a\,[\bar{T}(t_{\mathrm{shut}}) - \bar{T}(t_{\mathrm{start}})] + H_w. \tag{6}$$

The 3.59 kJ mean aperture integral exceeds the measured heating of the interior air by 0.03 kJ. This difference is small compared to the combined measurement uncertainty. It provides a residual on the opening-time budget without determining the heat path into individual liner and plate elements. A thermal response measured during closure includes air already warmed by exchange. Counting that recovery heat as a second heat input would double-count the same transfer.

TABLE II. Estimated systematic standard uncertainty in isolated-opening heat and in the 6 s heat ratio. Calibration and reduction terms enter once as common quantities where appropriate. Quadrature totals assume independent rows and exclude between-block repeatability.

Source	Q_1 (kJ)	$R(6\,\mathrm{s})$
Velocity and temperature gains	0.090	0.006
Spatial interpolation and mask	0.070	0.011
Edge and door-motion timing	0.060	0.010
Mass balance and density	0.050	0.012
Temperature response correction	0.030	0.002
Combined	0.14	0.020

The gain term is largest for the absolute load. Its effect mostly cancels in a ratio. At a short gap the two openings have different vertical density profiles, so the mass-balance and mask terms cancel only in part. At long gaps the perturbations in the two integrated fluxes have similar signs and relative sizes. We report repeatability separately to preserve the distinction between day-to-day variability and common sources of bias in the apparatus [20].

APPENDIX B: REPEATED-OPENING MAP

For a sequence of complete door events, let x_n^- and x_n^+ be the normalized temperature anomaly just before and just after opening n. If each event removes a fraction f of the remaining deficit, the intrusion raises the anomaly by $f(1 - x_n^-)$. A sealed interval Δ_n then gives

$$x_{n+1}^- = \exp(-\Delta_n/\tau)[f + (1 - f)x_n^-]. \tag{7}$$

The initial condition $x_1^- = 0$ recovers Eq. (4) for the second event. For a constant interval Δ put $a = \exp(-\Delta/\tau)$. The map has a contraction factor $a(1 - f)$ and an asymptotic deficit

$$1 - x_\infty^- = \frac{1 - a}{1 - a(1 - f)}. \tag{8}$$

Equation (8) follows by summing the geometric sequence of within-run carryover terms. For the fitted coefficients and a hypothetical fixed 6 s interval it gives 0.17 of the isolated load per event, compared with 0.48 at the second event. The steady limit assumes that the effective conductance and the temperature of the external supply stay fixed as warming accumulates. In a prolonged sequence, the liner would store heat and the external air that the incoming stream samples might retain a contribution from previous openings. The two-event observations test the first application of Eq. (7). They do not constrain the asymptotic heat.

APPENDIX C: BLOCK VALUES FOR THE PAIRED EXPERIMENT

Table III gives each isolated-opening heat to 0.01 kJ and each paired ratio to 0.01. For delay d, the interval in Table I follows from $\bar{r}_d \pm t_{0.975,11} s_d/\sqrt{12}$, where s_d is the sample standard deviation of the 12 daily ratios. The uncertainties reflect variation under the protocol for this apparatus. In particular, the 12 days are replicate initial conditions for the same cabinet and plate, and are not independent cabinets.

TABLE III. Daily sensible heat of an isolated opening and paired heat ratios. The last six columns identify the sealed interval in seconds.

Block	Isolated (kJ)	6	15	30	60	120	240
1	3.43	0.53	0.47	0.62	0.88	0.95	1.05
2	3.60	0.55	0.50	0.73	0.80	0.96	1.04
3	3.83	0.57	0.57	0.60	0.75	0.98	0.94
4	3.40	0.47	0.63	0.64	0.73	0.97	0.96
5	3.54	0.48	0.58	0.73	0.83	0.86	1.03
6	3.72	0.49	0.60	0.72	0.78	0.85	0.95
7	3.79	0.52	0.54	0.73	0.82	0.94	0.97
8	3.49	0.42	0.57	0.68	0.86	0.86	1.06
9	3.47	0.46	0.50	0.63	0.75	0.87	0.99
10	3.64	0.43	0.56	0.63	0.89	0.99	0.92
11	3.51	0.45	0.49	0.63	0.85	1.00	0.92
12	3.66	0.51	0.59	0.58	0.78	0.93	1.05

ACKNOWLEDGMENTS

We thank Inger Dahl-Kovač for rebuilding the cabinet seal and Masato Arai-Vidal for the aperture calibration jig.

[1] P. F. Linden, Annual Review of Fluid Mechanics **31**, 201 (1999).
[2] N. A. Engerer, D. J. Stensrud, and M. C. Coniglio, Monthly Weather Review **136**, 4839 (2008).
[3] T. B. Benjamin, Journal of Fluid Mechanics **31**, 209 (1968).
[4] J. O. Shin, S. B. Dalziel, and P. F. Linden, Journal of Fluid Mechanics **521**, 1 (2004).
[5] J. E. Simpson and R. E. Britter, Journal of Fluid Mechanics **94**, 477 (1979).
[6] W. G. Brown and K. R. Solvason, International Journal of Heat and Mass Transfer **5**, 859 (1962).
[7] P. Chen, D. J. Cleland, S. J. Lovatt, and M. R. Bassett, International Journal of Refrigeration **25**, 799 (2002).
[8] A. M. Foster, M. J. Swain, R. Barrett, and S. J. James, International Journal of Refrigeration **26**, 918 (2003).
[9] A. Tervonen-Imaz and A. Costa-Tuuli, *Position sensitivity of temperature probes in short-duration enclosure exchange*, Kivilahti Centre for Applied Metrology (2019).
[10] C. Savignac-Mena and N. Belhadri-Mercier, *Thermal relaxation of lined enclosures under pulse heating*, Institut de Veyrac (2021).
[11] P. F. Linden, G. F. Lane-Serff, and D. A. Smeed, Journal of Fluid Mechanics **212**, 309 (1990).
[12] W. D. Baines and J. S. Turner, Journal of Fluid Mechanics **37**, 51 (1969).
[13] G. R. Hunt and P. F. Linden, Building and Environment **34**, 707 (1999).
[14] M. Raffel, C. E. Willert, F. Scarano, C. J. Kähler, S. T. Wereley, and J. Kompenhans, *Particle Image Velocimetry: A Practical Guide* (Springer, 2018).
[15] B. Efron and R. J. Tibshirani, *An Introduction to the Bootstrap* (Chapman & Hall, 1993).
[16] T. H. Ellison and J. S. Turner, Journal of Fluid Mechanics **6**, 423 (1959).
[17] L. Imbert-Sagara and F. Malm-Ayadi, *Pressure and velocity transients across an isothermal swinging aperture*, Montvernet Institute for Building Physics (2020).
[18] L. Mahieu-Araya and A. Torvalds-Neri, *Event boundaries in paired measurements of enclosure infiltration*, Toftesund Technical Institute (2022).
[19] V. Rueda-Lakatos and N. Sarin-Kuroda, *Classification of household refrigerator use from door-state records*, Alderval Centre for Domestic Energy (2018).
[20] Joint Committee for Guides in Metrology, *Evaluation of measurement data: Guide to the expression of uncertainty in measurement*, Joint Committee for Guides in Metrology (2008).